2019

Numerical simulation of stress distribution in longwall panels during the first caving interval

Sadjad Mohammadi
Shahrood University of Technology, Iran

Mohammad Ataei
Shahrood University of Technology, Iran

Reza Kakaie
Shahrood University of Technology, Iran

Ali Mirzaghorbanali
University of Sothern Queensland

Naj Aziz
University of Wollongong, naj@uow.edu.au

See next page for additional authors

Publication Details

Sadjad Mohammadi, Mohammad Ataei, Reza Kakaie, Ali Mirzaghorbanali, Naj Aziz and Ashkan Rastegarmanesh, Numerical simulation of stress distribution in longwall panels during the first caving interval, in Naj Aziz and Bob Kininmonth (eds.), Proceedings of the 2019 Coal Operators Conference, Mining Engineering, University of Wollongong, 18-20 February 2019, 82-90.

NUMERICAL SIMULATION OF STRESS DISTRIBUTION IN LONGWALL PANELS DURING THE FIRST CAVING INTERVAL

Sadjad Mohammadi[1], Mohammad Ataei[2], Reza Kakaie[3], Ali Mirzaghorbanali[4], Naj Aziz[5] and Ashkan Rastegarmanesh[6]

ABSTRACT: Reliable prediction of induced stress distribution in longwall panels enhances safety in longwall mining. This paper presents the results of numerical simulation intended to examine stress distribution in terms of peak abutment pressures during the first caving of longwall mining. Longwall mining was simulated by incorporating Universal Distinct Element Code (UDEC). Several conceptual models were developed and subsequently analyzed to investigate the effects of five critical parameters on peak abutment pressures. Critical parameters that were studied as a part of this investigation included roof strata uniaxial compressive strength, immediate roof height, spacing of bedding planes and Vertical and horizontal *in situ* stresses. The results of numerical simulation increased the current understanding of rear and front abutment pressures in longwall *mining under various geo-mining conditions.*

INTRODUCTION

Study of the induced stress distributions in the vicinity of a longwall panel plays a fundamental role in the understanding of mining mechanics due to its direct impact on safety and productivity. The stress distribution in term of abutment pressures (Figure 1) has a direct effect on the failure mechanism, roof control, location and stability of the gateroads and frequency and intensity of dynamic accidents such as gas outburst and rockburst in working faces. Accordingly, the accurate prediction of the abutment pressures enhances safety in longwall mining.

There are direct (e.g. stress measurement, experimental simulation, simplified elastic–plastic or constitutional damage calculation) and indirect (e.g. tunnel deformation and support pressure measurement) methods to measure the abutment pressures (Gao *et al*., 2013). Up to now, several equations were presented in the literature to predict abutment pressures (Salamon, 1963; Peng and Chiang, 1984; Jeramic, 1985; Wilson, 1986; Mark, 1990; Heasley, 1998; Gil, 2013; Verma and Deb, 2013; Zhu *et al*., 2015). Furthermore, some other researchers have studied numerically the effect of various pertinent parameters on the abutment pressures (Singh and Singh, 2010; Gao *et al*., 2013; Ju *et al*., 2015; Ji *et al*., 2016; Jiang *et al*., 2018).

In the literature, no studies have been carried out to investigate the effects of critical parameters on the abutment pressures with regards to the existence of different strata in the immediate roof. It is noted that discontinuous methods are more appropriate for simulating the progressive caving of strata due to longwall mining. Accordingly, a systematic numerical study incorporating Universal Distinct Element Code (UDEC) was performed to investigate the effects of five critical parameters on the rear and front Peak Abutment Pressures (PAP) during the first caving interval considering the different composition of immediate roof strata. Critical parameters that

[1] *Ph.D. Shahrood University of Technology, Iran. Email: sadjadmohammadi@shahroodut.ac.ir*
[2] *Professor, Shahrood University of Technology, Iran. Email: ataei@shahroodut.ac.ir*
[3] *Professor, Shahrood University of Technology, Iran. Email: r_kakaie@shahroodut.ac.ir*
[4] *Senior lecturer, University of Sothern Queensland, Australia. Email: ali.mirzaghorbanali@usq.edu.au*
[5] *Professor, University of Wollongong, Australia. Email: naj@uow.edu.au*
[6] *Postgraduate researcher, University of Southern Queensland. Email: ashkan.rastegarmanesh@usq.edu.au*

were studied included the roof strata uniaxial compressive strength, immediate roof height, spacing of bedding planes and *in situ* stresses.

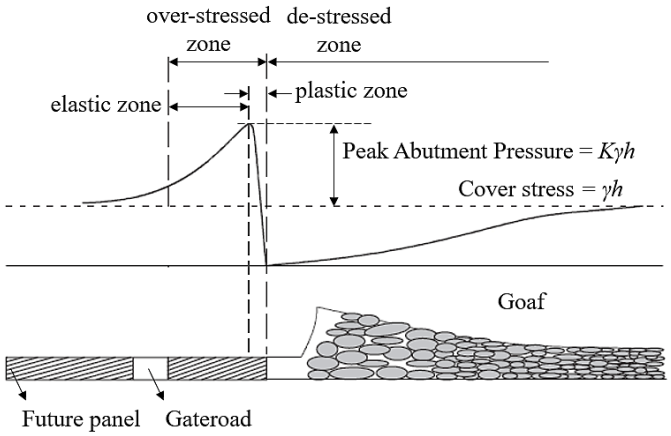

Figure 1: Abutment pressure state (modified from Yavuz, 2004)

SIMULATION REQUIREMENTS

The two-dimensional Universal Discrete Element Code (UDEC) was used to simulate the first caving event due to longwall mining. For this purpose, an *initial condition* was defined, then, to study each parameter, only the value of that particular parameter was changed and the other parameters were kept constant under the *initial condition*. Table 1 illustrates the *initial condition*. Geometry and boundary conditions of the constructed models are shown in Figure 2.

Table 1: Basic conditions

Parameters	Value
Coal seam thickness	2 m
Immediate roof height	5 m
Mining depth	300 m
In situstresses ratio	1
Bedding planes spacing	1 m
Number of cross joint	1
Joint set dip	90°
Joint set orientation	Parallel to the face
Joint set spacing	1 m
Joint set persistence	0.5 m

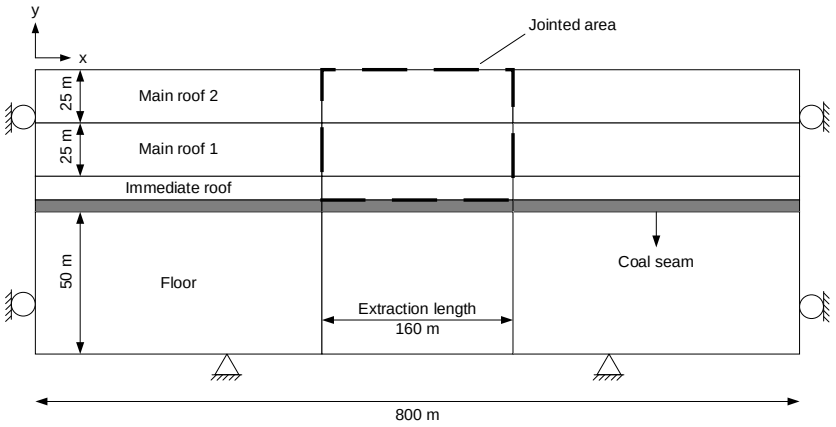

Figure 2: Geometry and boundary conditions of the numerical model

In order to consider a variety of strata in the immediate roof, four types of immediate roofs were studied as shown in Figure 3. These types have been selected in such a way that immediate roof strata that was weak, or strong or that various components could be considered.

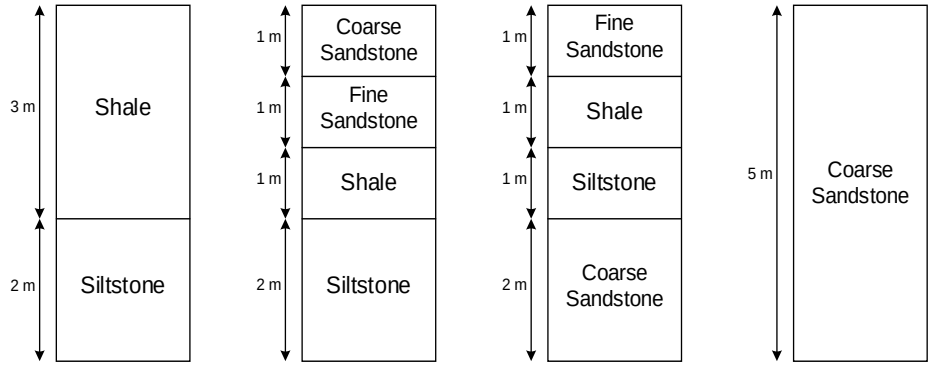

Figure 3: Four types of immediate roof

In the models, the rock blocks obey strain-softening (elastic-brittle-plastic) constitutive model with an ultimate and residual strength defined by modified Mohr-Coulomb strength criterion. Discontinuities follow Mohr-Coulomb constitutive law. The mechanical properties of the rock mass and discontinuities (Table 2 and Table 3) for this study were deduced from the mean of field data compiled for various panels and typical values extracted from the literature.

Table 2: Mechanical properties of rock blocks

Rock	σ_{ci} (MPa)	E (GPa)	ρ (kg/m^3)	ν	C (MPa)	φ (°)	ψ (°)	C_r (MPa)	φ_r (°)	ψ_r (°)
Siltstone	10.00	3.10	2600	0.25	2.21	37.07	5	0.22	24.71	3.33
Shale	36.00	11.16	2600	0.25	8.311	38.91	5	0.83	25.94	3.33
Fine Sandstone	75.00	23.25	2600	0.25	14.30	45.73	5	1.43	30.50	3.33
Coarse Sandstone	150.00	46.50	2600	0.25	28.61	45.73	5	2.86	30.50	3.33
Floor and main roofs	120.00	37.20	2600	0.25	24.20	43.00	5	2.42	28.67	3.33
Coal	15.00	2.00	1500	0.4	5.80	15.28	2	0.58	10.20	1.33

σ_{ci}: intact compressive strength; E: Young's modulus; ρ: density; ν: Poisson's ratio; C: cohesion; φ: angle of internal friction; ψ: angle of dilatancy; C_r: residual cohesion; φ_r: angle of residual internal friction; ψ_r: angle of residual dilatancy

Table 3: Mechanical properties of discontinuities

Parameters	C (Mpa)	φ (°)	σ_t (Mpa)	K_n (GPa/m)	K_s (GPa/m)
value	0	30	0	20	4

C: cohesion; φ: angle of internal friction; σ_t: tensile strength; K_n: normal stiffness; K_s: shear stiffness

RESULTS

Effect of strata UCS

The coal strata are grouped into several composite layers which have diverse thicknesses with different and complex mechanical and caving behaviour. Different strata properties have different influences on the immediate roof properties. Therefore, to consider the effect of such condition in overall strength of the immediate roof, the Equivalent Immediate Roof Strength (EIRS) was defined as the thickness-weighted average of the roof strata uniaxial compressive strength as follows:

$$EIRS = \frac{\sum_{i=1}^{n} t_i \times \sigma_{c_i}}{\sum_{i=1}^{n} t_i} \quad (1)$$

where t_i is the thickness of the ith stratum (m), σ_{c_i} is the Uniaxial Compressive Strength (UCS) of the i^{th} stratum (MPa), and n is the number of stratum within the immediate roof.

Figure 4 shows the results of PAPs modelling for the studied roofs (in which its EIRS are 25.6, 56.2, 84.2, and 150 MPa, respectively) in the initial condition.

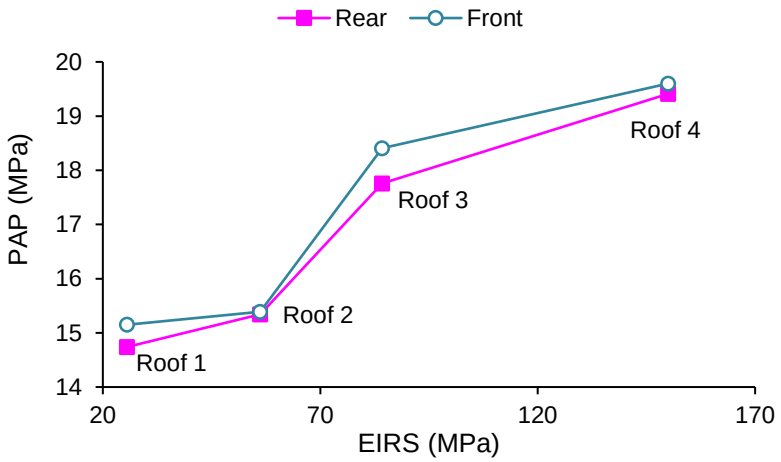

Figure 4: Peak abutment pressures versus EIRS of immediate roof

From Figure 4 it is concluded that an increase in the overall strength of the immediate roof (EIRS) produces higher PAPs. The findings show that the front PAP increased from 15.15 MPa to 19.60 MPa with an increase in EIRS from 25.60 to 150 MPa. The rear PAP inhabits a similar trend, in which PAP varies from 14.74 MPa to 19.41 MPa. Moreover, it is observed that the rear PAP is always less than the front one.

Effect of immediate roof height

The immediate roof height (which is usually equal to the caving height) is correlated with extraction height as followS:

$$h_{im} = \frac{m}{K-1} \quad (2)$$

where m is the extraction height (m) and K is the bulking factor of immediate roof.

Peng and Chiang (1984), based on field investigations, stated that the bulking factor of coal measure rocks varied between 1.1 and1.5. Shabanimashcool (2012), based on the available literature, proved that the porosity of caved materials is approximately 0.3 which corresponds to a bulking factor of 1.43. Consequently, the immediate roof height would be roughly 2.5 times the extraction height which is also the assumed value in this study. Accordingly, in order to investigate the effect of the immediate roof on the PAPs, three heights (5, 7.5, and 12.5) were considered (Figure 5).

Contingent upon Figure 5, it is noted that there is a decreasing trend in the rear and front PAPs with an increase in immediate roof height, and supposedly, an exponential decay function could describe the decreasing trend of the PAPs with respect to immediate roof height for all of the studied roofs. Moreover, it is evident that the gradient of the trend line in strong roofs (roof 3 and 4) is higher than that of the weak roofs (roof 1 and 2).

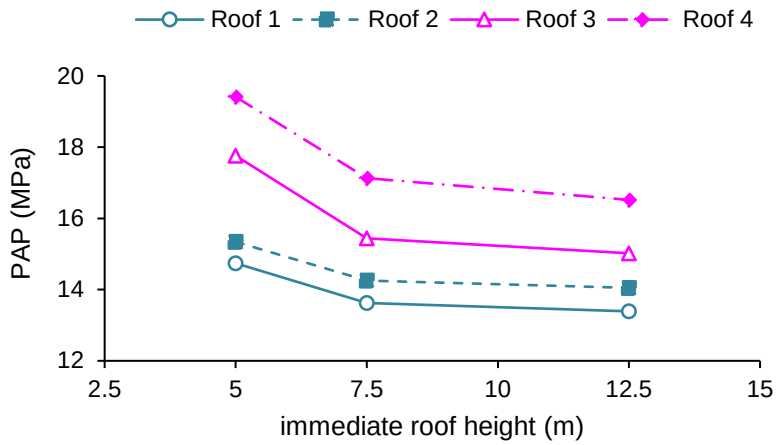

a. rear PAP

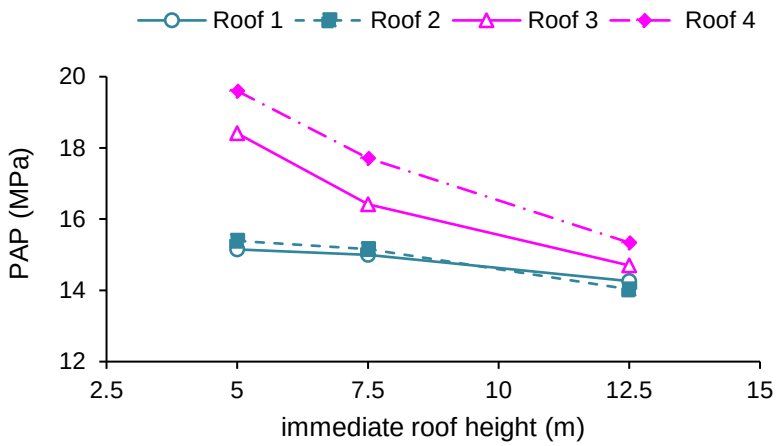

b. front PAP

Figure 5: Peak abutment pressures versus immediate roof height

Effect of bedding planes spacing

The bedding planes in the immediate roof were simulated by horizontal persistent joints with three mean spacing (0.25, 0.5, and 1 m). It is noted that the bedding planes spacing was presumed constant in the entire immediate roof. The bedding planes influence on the PAPs is illustrated in Figure 6.

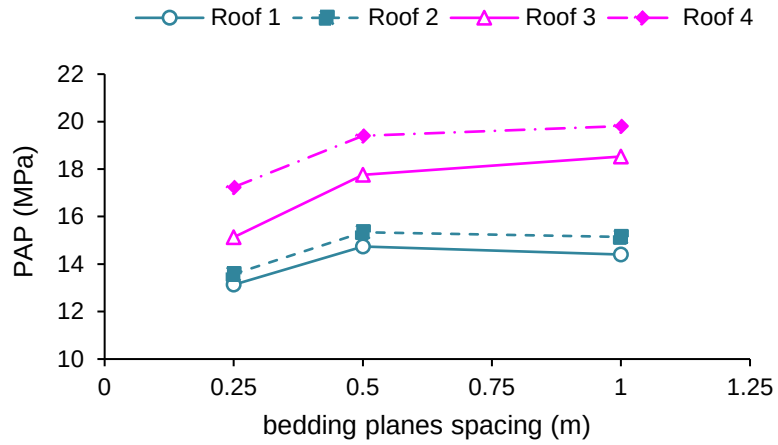

a. rear PAP

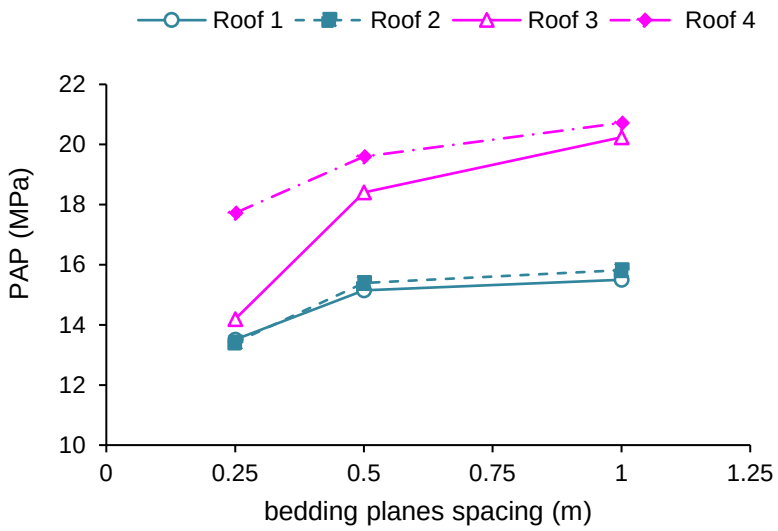

b. front PAP

Figure 6: Peak abutment pressures versus bedding planes spacing

According to Figure 6, the rear and front PAPs observed during first caving event show an increasing trend with increases in the mean spacing of bedding planes and furthermore, the relationship between PAPs and bedding planes spacing is of a logarithmic growth. In addition, it is also clear that the growth rate of the strong roofs (roof 3 and 4) are higher than that of the weak roofs (roof 1 and 2).

Effect of vertical in situstress

A parametric study to assess the effect of *in situ* stress on the PAPs was done by varying mining depth. Accordingly, a simulation was performed using four depths values of 150, 300, 600, and 1000 meters which corresponds to vertical *in situs* tresses of 2.6, 6.5, 14.3 and 24.7 MPa (Figure 7).

Plots in Figure 7 show that the rear and front PAPs increases almost linearly with an increase in strata depth and consequently vertical *in situ* stress. Additionally, the graphs show that both PAPs increases drastically with increase in strata depth up to a value of 600 meters, however, when the depth of working increases to 1000 m, the PAPs increases gradually as well.

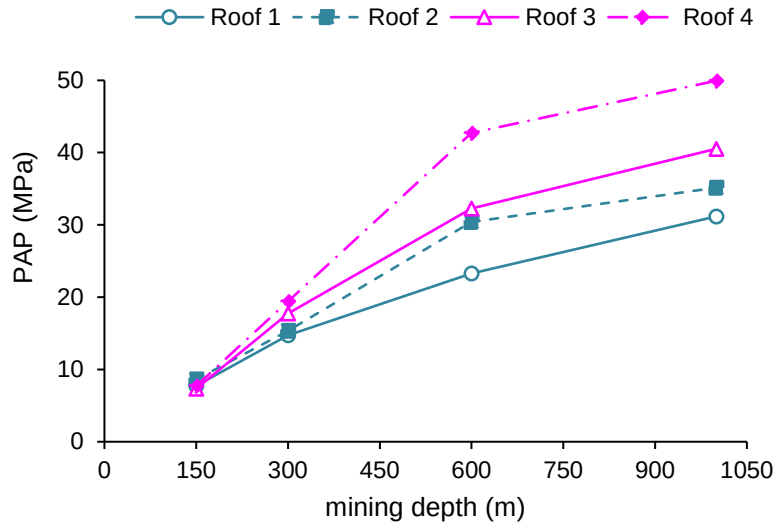

a. rear PAP

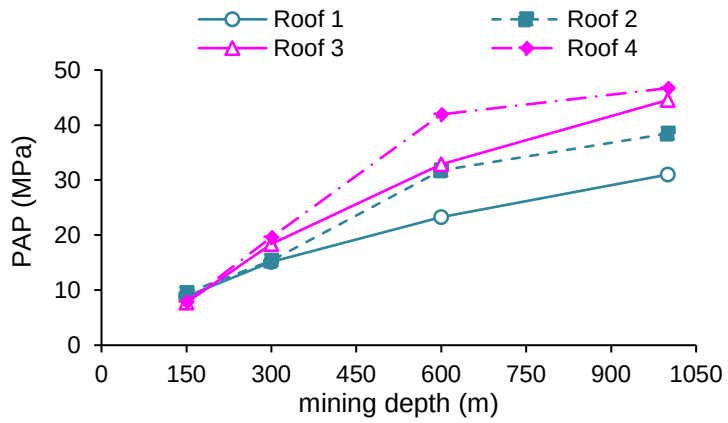

b. front PAP

Figure 7: Peak abutment pressures versus vertical in situ stress

Effect of horizontal in situ stress

Finally, the effect of the horizontal *in situ* stress on the PAPs was conducted via using a parametric study of different *in situ* stress ratios (*K*). For this purpose, strata depth of 300 meters was assumed and *K* was changed from 0.5 to 3 which correspond to a band of 3.25 to 19.5 MPa of horizontal *in situ* stress change (Figure 8).

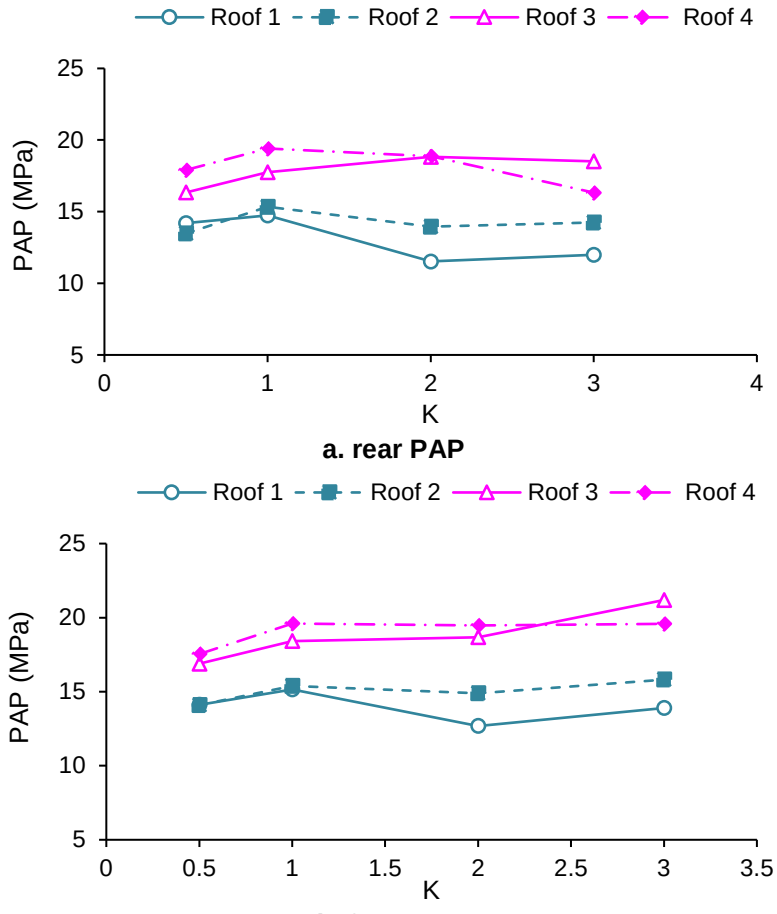

a. rear PAP

b. front PAP

Figure 8: Peak abutment pressures versus horizontal in situstress

Figure 8 illustrates there is no clear relationship between PAPs and the horizontal in situstress. These results show that while the horizontal in situstress increases, both rear and front PAPs

fluctuate capriciously. Furthermore, the magnitude of the rear and front PAPs in strong roofs are always higher than that of the weak roofs irrespective of the horizontal in situstress value.

DISCUSSION

The prime motivation for this study was to investigate the relationship between the rear and front abutment pressures and some critical parameters. Different types of roofs in terms of strength and composition were taken into account while incorporating discontinuous by numerical modelling. Undoubtedly, the obtained values are not applicable to all cases, however, the general trends of the relationships are valid.

Figure 4 showed that there is a direct relationship between *EIRS* and PAPs. This relationship should be interpreted by taking the first caving interval into consideration. The effect of an increase in *EIRS* is an increase in the first caving interval. Consequently, based on the principals of potential energy balance, the PAPs are higher. Later, the indirect relationship between the immediate roof height and PAPs could be inferred from Figure 5. This result is in line with the analytical results of Majumder and Chakrabarty (1991) and numerical findings of Singh and Singh (2010). Moreover, Figure 6 indicated that the result of an increase in the bedding planes spacing would be higher PAPs which reflect the direct correlation between these two variables. This finding confirms the results of the numerical modelling of Gao *et al*. (2014). In addition, a direct relationship between the vertical in situstress (which corresponds to strata depth) and PAPs is concluded from Figure 7 which is in accordance with the findings of Singh and Singh (2010). Meanwhile, the PAPs and main caving span are not always correlated directly and it is necessary to take into account the working depth. In a constant depth, an increase in the main caving span of a given roof is encountered with an increase in PAPs (similar to the interpretation of the results of the effect of strata UCS). Nevertheless, when the mining depth increases, the main caving span decreases, however, PAPs will be higher. Figure 8 showed there is not a clear relationship between the *horizontal in situ stress* and PAPs. This result is inconsistent with the numerical modelling results of Singh and Singh (2010). Gao *et al*. (2014) discussed that the most significant influence of horizontal stress is changes in the fracture mechanism in the immediate roof from bed bending failure to bed shear fracture which results in changing the main caving span. This phenomenon could be one of the reasons for fluctuation in the PAPs. Moreover, in this paper, the direction of principal horizontal *in situ* stress was deliberately taken parallel to the panel length which could impact on the induced stress pattern in turn. However, to achieve a realistic and clearer explanation, a 3-D simulation is necessary.

CONCLUSIONS

Results of numerical simulation to investigate the effect of some critical parameters on the peak abutment pressures with the help of UDEC software were presented. The following main conclusions are extracted from this study:

- The front peak abutment pressure is always higher than the rear one.
- Equivalent strength of immediate roof (EIRS), average spacing of bedding planes in the immediate roof strata and the vertical *in situ* stress have a direct relationship with the rear and front abutment pressures whereas this relationship is indirect for the immediate roof height and the extraction height.
- All recognized relationships are almost linearly with the exception of bedding planes spacing and the immediate roof height which are logarithmic growth and exponential decay, respectively.

- The obtained results showed that there is no clear relationship between the horizontal *in situ* stress and the peak abutment pressures. This should be further scrutinized through 3-D simulations.

REFERENCES

Gao, M, Jin, W, Dai, Z and Xie, J, 2013. Relevance between abutment pressure and fractal dimension of crack network induced by mining. *International Journal of Mining Science and Technology*, *23*(6): 925-930.

Gil, H, ed., 2013. *The theory of strata mechanics* (Vol. 63) (Elsevier)

Heasley, K A, 1998. Numerical modeling of coal mines with a laminated displacement-discontinuity code. PhD thesis, Colorado School of Mines.

Jeremic, M, 1985. Strata mechanics in coal mining (CRC Press)

Ji, Y, Wang, X, Zhou, Y and Zhang, X, 2016. Study on the Distribution Law of Front Abutment Pressure of Long Fully-Mechanized Working Face in Deep Mine. In *Coal in the 21st Century: Mining, Processing and Safety*, pp 159-162.

Jiang, J Q, Wu, Q S, Wu, Q L, Wang, P, Zhang, C and Gong, B, in press. Study on Distribution Characteristics of Mining Stress and Elastic Energy Under Hard and Thick Igneous Rocks. *Geotechnical and Geological Engineering*.

Ju, M H, Li, X H, Yao, Q L, Li, D W, Chong, Z H and Zhou, J, 2015. Numerical investigation into effect of rear barrier pillar on stress distribution around a longwall face. *Journal of Central South University*, *22*(11): 4372-4384.

Majumder, S and Chakrabarty, S, 1991. The vertical stress distribution in a coal side of a roadway—an elastic foundation approach. *Mining Science and Technology*, *12*(3): 233-240.

Mark, C, 1990. Pillar design methods for longwall mining. US Department of the Interior, Bureau of Mines.

Peng, S S and Chiang, H S, 1984. Longwall mining (Wiley: New York)

Salamon, M G D, 1963. Elastic analysis of displacements and stresses induced by the mining of seam or reef deposits. *Journal of the Southern African Institute of Mining and Metallurgy*, *64*(4): 128-149.

Shabanimashcool, M, 2012. Numerical modelling of the longwall mining and the stress state in Svea Nord Coal Mine, PhD thesis, Norwegian University of Science and Technology, Trondheim.

Singh, G S P and Singh, U K, 2010. Numerical modeling study of the effect of some critical parameters on caving behavior of strata and support performance in a longwall working. *Rock Mechanics and Rock Engineering*, *43*(4): 475-489.

Verma, A K and Deb, D, 2013. Numerical analysis of an interaction between hydraulic-powered support and surrounding rock strata. *International Journal of Geomechanics*, *13*(2): 181-192.

Wilson, A H, 1986. The problems of strong roof beds and water bearing strata in the control of longwall faces. In *Proceedings of symposium on ground movement and control related to coal mining (Organized by the Australian Institute of Mining and Metallurgy, Illawara Branch, University of Wollongong)* (pp. 1-8).

Yavuz, H, 2004. An estimation method for cover pressure re-establishment distance and pressure distribution in the goaf of longwall coal mines. *International Journal of Rock Mechanics and Mining Sciences*, *41*(2): 193-205.

Zhu, S, Feng, Y and Jiang, F, 2016. Determination of abutment pressure in coal mines with extremely thick alluvium stratum: a typical kind of rockburst mines in China. *Rock Mechanics and Rock Engineering*, *49*(5): 1943-1952.